Communication

Establishment of Anti-Dog PD-L1 Monoclonal Antibodies for Immunohistochemistry

Tsunenori Ouchida [1], Hiroyuki Suzuki [1,2,*], Tomohiro Tanaka [2], Mika K. Kaneko [1,2] and Yukinari Kato [1,2,*]

[1] Department of Antibody Drug Development, Tohoku University Graduate School of Medicine, 2-1 Seiryo-machi, Aoba-ku, Sendai 980-8575, Miyagi, Japan; tsunenori.ouchida.d5@tohoku.ac.jp (T.O.); k.mika@med.tohoku.ac.jp (M.K.K.)

[2] Department of Molecular Pharmacology, Tohoku University Graduate School of Medicine, 2-1 Seiryo-machi, Aoba-ku, Sendai 980-8575, Miyagi, Japan; tomohiro.tanaka.b5@tohoku.ac.jp

* Correspondence: hiroyuki.suzuki.b4@tohoku.ac.jp (H.S.); yukinari.kato.e6@tohoku.ac.jp (Y.K); Tel.: +81-22-717-8207 (H.S.&Y.K)

Abstract: Immune checkpoint blockade therapy has shown successful clinical outcomes in multiple human cancers. In dogs, several types of tumors resemble human tumors in many respects. Therefore, several groups have developed the anti-dog programmed cell death ligand 1 (dPD-L1) monoclonal antibodies (mAbs) and showed efficacy in several canine tumors. To examine the abundance of dPD-L1 in canine tumors, anti-dPD-L1 diagnostic mAbs for immunohistochemistry are required. In this study, we immunized the peptide in the dPD-L1 intracellular domain, and established anti-dPD-L1 mAbs, L$_1$Mab-352 (mouse IgG$_1$, kappa) and L$_1$Mab-354 (mouse IgG$_1$, kappa). In enzyme-linked immunosorbent assay, L$_1$Mab-352 and L$_1$Mab-354 showed high binding affinity to the dPD-L1 peptide, and the dissociation constants (K_D) were determined as 6.9×10^{-10} M and 7.2×10^{-10} M, respectively. Furthermore, L$_1$Mab-352 and L$_1$Mab-354 were applicable for the detection of dPD-L1 in immunohistochemical analysis in paraffin-embedded dPD-L1-expressed cells. These results indicated that L$_1$Mab-352 and L$_1$Mab-354 are useful for detecting dPD-L1 in immunohistochemical analysis.

Keywords: dPD-L1; monoclonal antibody; peptide immunization; immunohistochemistry

1. Introduction

Immune checkpoint blockade therapy has recently revolutionized the treatment and clinical outcome of several cancer types [1]. The therapies targeting programmed cell death 1 (PD-1), programmed cell death ligand 1 (PD-L1), and cytotoxic T-lymphocyte-associated antigen 4 (CTLA-4) have become the standard therapy for several human tumors. The therapeutic mAbs against PD-1 receptor (nivolumab and pembrolizumab), PD-L1 (atezolizumab, durvalumab, and avelumab), CTLA-4 (tremelimumab and ipilimumab) were approved by Food and Drug Administration (FDA) [2]. These mAbs have been used in either monotherapy or combinatorial therapy with chemotherapy, radiation therapy, or other modalities [1]. These antibodies improve the response rates, progression-free survival, and overall survival in patients with various types of cancers [3–5].

PD-L1 (CD274) is a type I membrane protein expressed on non-lymphoid cells and a ligand of PD-1 [6,7]. PD-1 plays a critical role in the negative regulation of immune cells including cytotoxic T lymphocyte (CTL) and is important for antitumor immunity. CTLs are activated by recognizing presented antigens by T cell receptor (TCR)-CD3 complex [8]. After the recognition, zeta-chain associated protein kinase (ZAP-70) is recruited to the TCR-CD3 complex and phosphorylated by lymphocyte protein tyrosine kinase, which transduces the downstream signaling [9,10]. In contrast, SH2-containing protein tyrosine phosphatase-2 (SHP-2) is recruited to PD-1 stimulated with PD-L1 [11]. Since SHP-2 dephosphorylates phosphorylated ZAP-70, PD-1 can inhibit the activation signals in CTLs.

 doi:10.20944/preprints202308.0725.v1

With the increase in life span in both humans and dogs, the cancer incidence has increased as well [12]. Several naturally occurring tumors in dogs resemble human tumors in many respects. Therefore, the research on canine tumor therapy can generate knowledge that informs and prioritizes new tumor therapy in humans.

The development of dog PD-L1 (dPD-L1) mAbs has been reported [13–17]. Using a canine chimeric mAb targeting PD-L1, tumor regression of undifferentiated sarcoma and oral melanoma was achieved [14,16,17]. On the other hand, tumors that did not respond to the treatment also existed. Furthermore, the combination therapy of anti-dPD-L1 mAbs with hypofractionated radiotherapy is more effective to prolong overall survival [18]. Therefore, the development of anti-dPD-L1 mAbs for diagnostic use is essential for the improvement of efficacy.

In this study, we established anti-dog PD-L1 (dPD-L1) mAbs (L_1Mab-352 and L_1Mab-354) by peptide immunization and showed the usefulness of the mAbs for immunohistochemical analysis in paraffin-embedded PD-L1-positive cells.

2. Materials and Methods

2.1. Preparation of cell lines

Chinese hamster ovary (CHO)-K1 and P3X63Ag8U.1 (P3U1) cells were obtained from the American Type Culture Collection (Manassas, VA).

The synthesized DNA (Eurofins Genomics KK, Tokyo, Japan) encoding signal sequence of N-terminus ($_{1}$-MRMFSVFTFMAYCHLLKA-$_{18}$) deleted dPD-L1 (dPD-L1, Accession No.: NM_001291972) was subsequently subcloned into a pCAGzeo_ssPA16 vector (IL2-signal sequence and PA16 tag added to N-terminus of construct). The amino acid sequence of the tag system was as follows: PA16 tag [19–22], sixteen amino acids (GLEGGVAMPGAEDDVV). The PA16 tag can be detected by an anti-human podoplanin mAb (clone NZ-1) [19–35]. The dPD-L1 plasmid was transfected into CHO-K1 cells, using a Neon transfection system (Thermo Fisher Scientific Inc., Waltham, MA). Stable transfectants were established through cell sorting using a cell sorter (SH800; Sony Corp., Tokyo, Japan), after which cultivation in a medium, containing 0.5 mg/mL of Zeocin (InvivoGen, San Diego, CA) was conducted.

CHO-K1, PA16-dPD-L1-overexpressed CHO-K1 (CHO/dPD-L1) and P3U1 cells were cultured in a Roswell Park Memorial Institute (RPMI)-1640 medium (Nacalai Tesque, Inc., Kyoto, Japan), with 10% heat-inactivated fetal bovine serum (FBS; Thermo Fisher Scientific Inc.), 100 units/mL of penicillin, 100 μg/mL of streptomycin, and 0.25 μg/mL of amphotericin B (Nacalai Tesque, Inc.). All cells were grown in a humidified incubator at 37°C, in an atmosphere of 5% CO_2 and 95% air.

2.2. Production of hybridomas

A five-week-old BALB/c mouse was purchased from CLEA Japan (Tokyo, Japan). The animal was housed under specific pathogen-free conditions. All animal experiments were approved by the Animal Care and Use Committee of Tohoku University (Permit number: 2022MdA-001). The dPD-L1 peptide ($_{260}$-KKHGRMMDVEKC-$_{271}$) and keyhole limpet hemocyanin-conjugated dPD-L1 peptide (dPD-L1 peptide-KLH) were purchased from Eurofins Japan.

To develop mAbs against dPD-L1, we intraperitoneally immunized one mouse with the dPD-L1 peptide-KLH (100 μg) plus Imject Alum (Thermo Fisher Scientific, Inc.). The procedure included three additional injections every week (100 μg), which were followed by a final booster intraperitoneal injection (100 μg), two days before harvesting splenocytes. The harvested splenocytes were subsequently fused with P3U1 cells, using PEG1500 (Roche Diagnostics, Indianapolis, IN). For the hybridoma selection, cells were cultured in the RPMI-1640 medium with 10% FBS, 100 units/mL of penicillin, 100 μg/mL of streptomycin, 0.25 μg/mL of amphotericin B, 5 μg/mL of Plasmocin, 5% Briclone (NICB, Dublin, Ireland), and hypoxanthine, aminopterin and thymidine (HAT; Thermo Fisher Scientific, Inc.). The supernatants were subsequently screened using enzyme-linked immunosorbent assay (ELISA) using the dPD-L1 peptide.

 doi:10.20944/preprints202308.0725.v1

2.3. Purification of mAbs

The cultured supernatants of L1Mab-352 and L1Mab-354-producing hybridomas were filtrated with Steritop (0.22 μm, Merck KGaA, Darmstadt, Germany). The filtered supernatants were subsequently applied to 1 mL of *Ab-Capcher ExTra* (ProteNova, Inc., Kagawa, Japan). After washing with phosphate-buffer saline (PBS), bound antibodies were eluted with an IgG elution buffer (Thermo Fisher Scientific, Inc.), followed by immediate neutralization of eluates, using 1M Tris-HCl (pH 8.0). Finally, the eluates were concentrated, after which PBS was replaced with the elution buffer using Amicon Ultra (Merck KGaA).

2.4. ELISA

The dPD-L1 peptide was immobilized on Nunc Maxisorp 96-well immunoplates (Thermo Fisher Scientific, Inc.) at 1 μg/mL for 30 minutes at 37°C. After washing with PBS containing 0.05% Tween20 (PBST; NacalaiTesque, Inc.), wells were blocked with 1% bovine serum albumin (BSA) in PBST for 30 minutes at 37°C. Then, plates were incubated at 1 μg/mL of L1Mab-352 and L1Mab-354, followed by peroxidase-conjugated anti-mouse immunoglobulins (1:1000; Agilent Technologies, Inc., Santa Clara, CA). Finally, enzymatic reactions were conducted using the ELISA POD substrate TMB kit (Nacalai Tesque, Inc.) and stopped by the addition of 1M H_2SO_4. The absorbance at 450 nm was measured by using an iMark microplate reader (Bio-Rad Laboratories, Inc., Berkeley, CA).

To determine the dissociation constant (K_D), L1Mab-352 and L1Mab-354 were serially diluted from 40 μg/mL to 2.4 ng/mL. The K_D was calculated by fitting saturation binding curves to the built-in; one-site binding models in GraphPad PRISM 8 (GraphPad Software, Inc., La Jolla, CA).

2.5. Flow cytometric analysis

CHO-K1 and CHO/dPD-L1 cells were harvested after a brief exposure to 0.25% trypsin and 1 mM ethylenediaminetetraacetic acid (EDTA, Nacalai Tesque, Inc.). The cells were subsequently washed with 0.1% BSA in PBS and treated with 1 μg/mL NZ-1 for 30 min at 4°C. The cells were treated with 2 μg/mL Alexa Fluor 488-conjugated anti-rat IgG (Cell Signaling Technology, Inc., Danvers, MA). The fluorescence data were collected using the EC800 Cell Analyzer (Sony Corp.).

2.6. Immunohistochemical analysis of paraffin-embedded CHO/dPD-L1

Cell blocks were produced using iPGell (Genostaff Co., Ltd., Tokyo, Japan). To deparaffinize, rehydrate and retrieve antigen, the sections were autoclaved in EnVision FLEX Target Retrieval Solution, High pH (high pH; #DM828, Agilent Technologies, Inc.) at 121°C for 20 minutes. Then, sections were blocked using the Super Block T20 (PBS) Blocking Buffer (Thermo Fisher Scientific, Inc.), incubated with 50 μg/mL L1Mab-352 or L1Mab-354 for 1 h at room temperature, and treated with the Envision + Kit for mouse (Agilent Technologies, Inc.) for 30 min. Finally, color was developed using 3,3′-diaminobenzidine tetrahydrochloride (DAB; Agilent Technologies, Inc.) for 5 min, and counterstaining was performed using hematoxylin (FUJIFILM Wako Pure Chemical Corporation, Osaka, Japan).

To inhibit L1Mab-352 and L1Mab-354 binding, dPD-L1 peptide (final concentration: 20 μg/mL) was mixed with L1Mab-352 or L1Mab-354 (final concentration: 50 μg/mL). After incubation for 1.5 h at room temperature, immunohistochemical analysis was performed.

3. Results

3.1. Establishment of novel dPD-L1 mAs.

For this study, we immunized a mouse with a KLH-conjugated synthetic peptide corresponding to an intracellular region of dPD-L1. To produce hybridomas, the splenocytes from the mouse were fused with P3U1 cells by using polyethylene glycol. The wells which reacted with the synthetic peptide were selected by ELISA. After limiting dilution and additional screening, two clones L1Mab-352 (mouse IgG_1, kappa) and L1Mab-354 (IgG_1, kappa) were finally established (Figure 1).

Preprints (www.preprints.org) | NOT PEER-REVIEWED | Posted: 9 August 2023 doi:10.20944/preprints202308.0725.v1

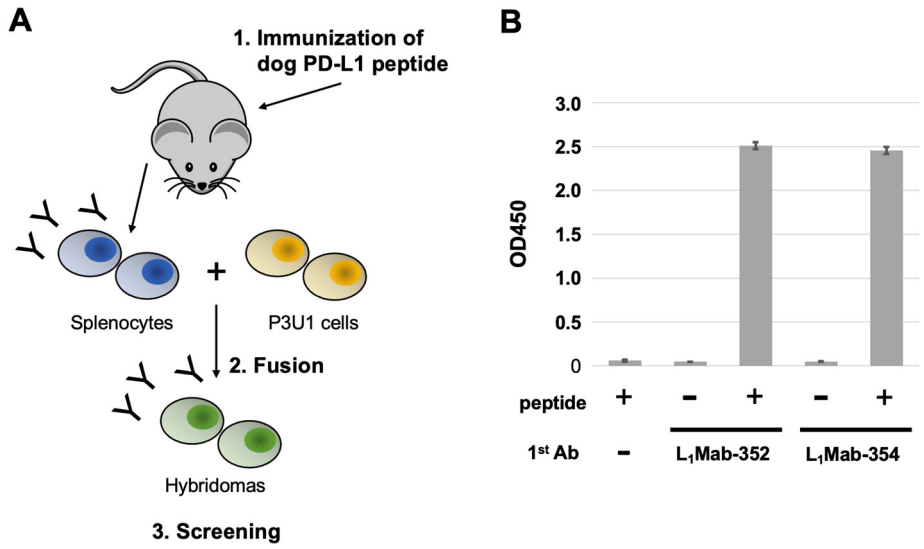

Figure 1. Establishment of novel dPD-L1 mAbs, L1Mab-352 and L1Mab-354. (**A**) The workflow of the establishment of L1Mab-352 and L1Mab-354. First, dPD-L1 peptide conjugated with KLH was immunized into a mouse. The splenocytes were then fused with P3U1 cells. After six days, hybridoma supernatants were selected by ELISA. (**B**) Synthesized peptides of dPD-L1 peptide (1 μg/mL) were immobilized on immunoplates for 30 min at 37℃. The plates were incubated with 1 μg/mL of L1Mab-352 and L1Mab-354, followed by the treatment of peroxidase-conjugated anti-mouse immunoglobulins. Optical density was measured at 450 nm (OD450) using a microplate reader. Error bars represent means ± SDs (n = 3).

3.2. Kinetic analyses of L1Mab-352 and L1Mab-354 against the dPD-L1 peptide.

To determine the K_D of L1Mab-352 and L1Mab-354 with the dPD-L1 peptide, we conducted the kinetic analysis using ELISA. After immobilization of the dPD-L1 peptide on immunoplates, serially diluted L1Mab-352 and L1Mab-354 were added. The mean of the absorbance at 450 nm was plotted versus the concentrations of L1Mab-352 and L1Mab-354. The K_D values of L1Mab-352 and L1Mab-354 for the dPD-L1 peptide were calculated as 6.9 ×10^{-10} M and 7.2 ×10^{-10} M, respectively (Figure 2).

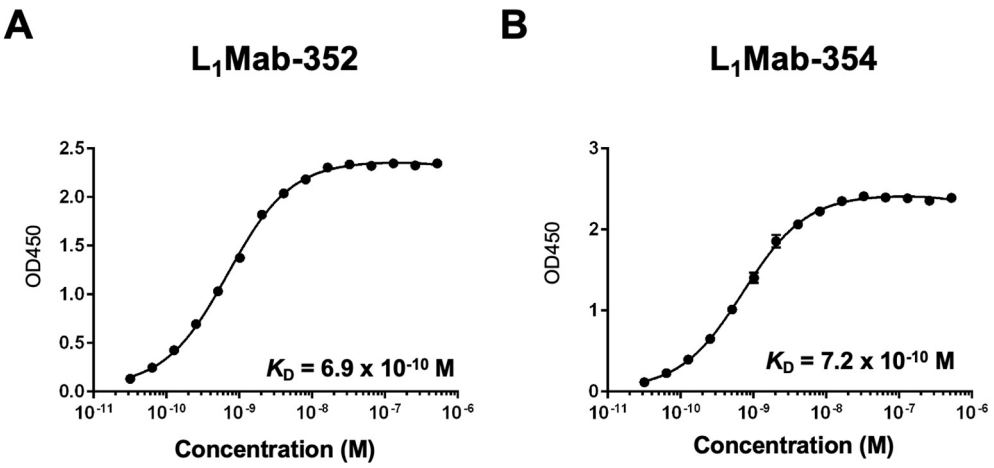

Figure 2. The determination of the binding affinity of L1Mab-352 and L1Mab-354 by ELISA. Synthesized peptides of dPD-L1 peptide (1 μg/mL) were immobilized on immunoplates for 30 min at 37°C. The plates were incubated with L1Mab-352 (**A**) and L1Mab-354 (**B**) at 2.4 ng/mL–40 μg/mL., followed by the treatment of peroxidase-conjugated anti-mouse immunoglobulins. Optical density was measured at 450 nm (OD450) using a microplate reader. The dissociation constant (K_D) was calculated using GraphPad PRISM 8. Error bars represent means ± SDs (n = 3).

Preprints (www.preprints.org) | NOT PEER-REVIEWED | Posted: 9 August 2023 doi:10.20944/preprints202308.0725.v1

3.3. Immunohistochemical analysis of L1Mab-352 and L1Mab-354 using paraffin-embedded CHO/dPD-L1.

We next performed immunohistochemical analysis against paraffin-embedded CHO/dPD-L1 cells (Figure 3A) using L1Mab-352 and L1Mab-354. We first confirmed the cell surface expression of dPD-L1 using flow cytometry (Figure 3B). Then, we prepared the paraffin-embedded CHO-K1 and CHO/dPD-L1 cells, and stained the section using L1Mab-352 and L1Mab-354. As shown in Figure 3C,D, L1Mab-352 and L1Mab-354 stained to the section of CHO/dPD-L1, but not that of CHO-K1. These results indicated that L1Mab-352 and L1Mab-354 can stain dPD-L1 in paraffin-embedded samples.

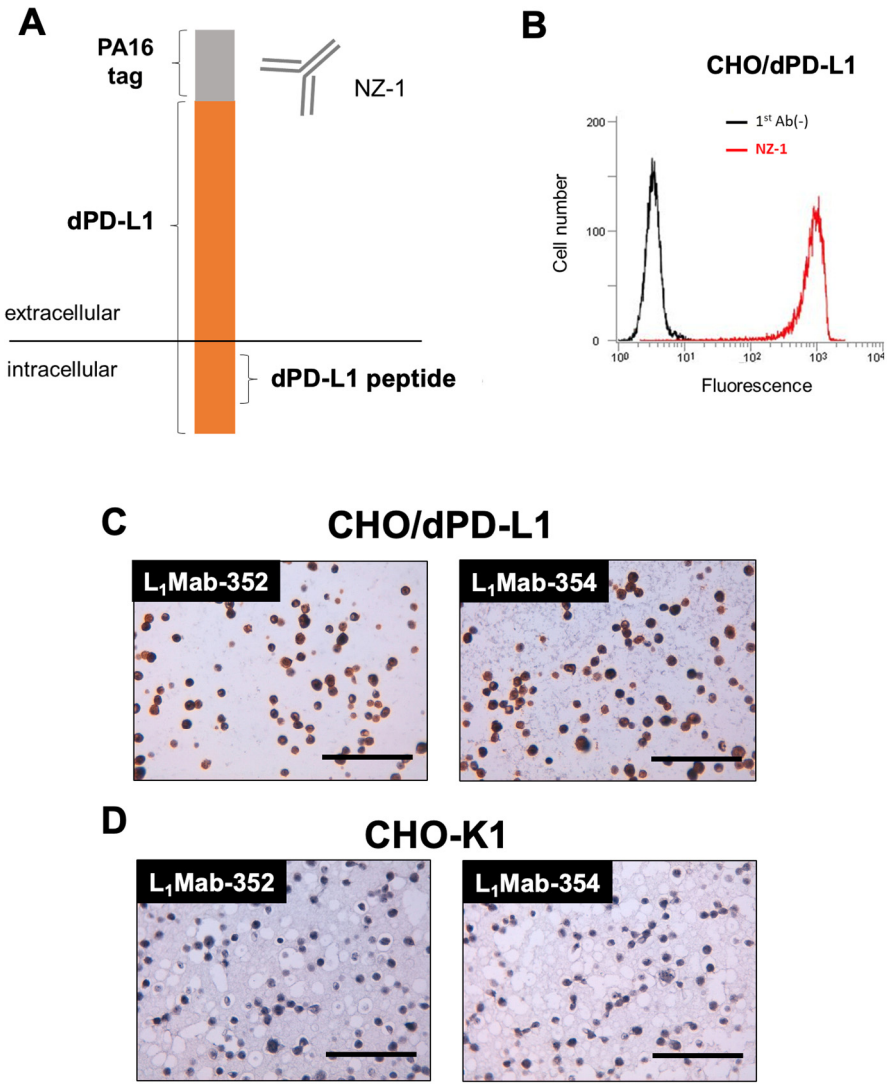

Figure 3. Immunohistochemical staining of paraffin-embedded CHO/dPD-L1 with L1Mab-352 and L1Mab-354. (**A**) The construction of dPD-L1. PA16 tag, the epitope of NZ-1, was tagged to the N-terminus of dPD-L1. The dPD-L1 peptide is located in the intracellular domain. (**B**) The cell surface expression of dPD-L1 was confirmed by flow cytometry using NZ-1. Red line: NZ-1. Black line: negative control. (**C**,**D**) Immunohistochemical analysis of paraffin-embedded CHO/dPD-L1 (**C**) and CHO-K1 (**D**) using 50 μg/mL of L1Mab-352 and L1Mab-354. Scale bar = 100 μm.

3.4. Peptide blocking of L1Mab-352 and L1Mab-354 in Immunohistochemical anayisis.

To confirm the specificity, we performed peptide blocking in the immunohistochemical analysis. As shown in Figure 4, the reactivity of L1Mab-352 and L1Mab-354 was blocked in the presence of dPD-L1 peptide. This result indicated that the signals of staining with L1Mab-352 and L1Mab-354 are caused by the specific binding to dPD-L1.

Preprints (www.preprints.org) | NOT PEER-REVIEWED | Posted: 9 August 2023 doi:10.20944/preprints202308.0725.v1

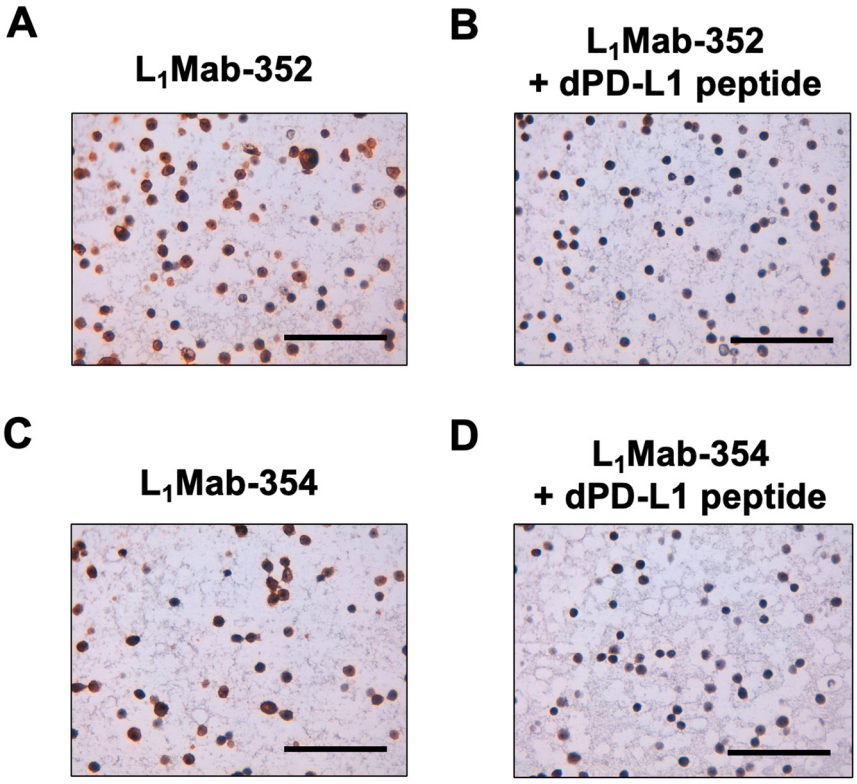

Figure 4. The blockade of L1Mab-352 and L1Mab-354 reactivity by dPD-L1 peptide. Immunohistochemical staining of paraffin-embedded CHO/dPD-L1 with L1Mab-352 (50 μg/mL) (**A**), L1Mab-352 (50 μg/mL) plus dPD-L1 peptide (20 μg/mL) (**B**), L1Mab-354 (50 μg/mL) (**C**), and L1Mab-354 plus dPD-L1 peptide (20 μg/mL) (**D**). Scale bar = 100 μm.

4. Discussion

Immune checkpoint blockade therapies have improved the patients' outcomes with various types of tumors [36]. However, only 30% of patients receive the benefit from the therapy [37]. Immunohistochemistry analyses to determine the PD-L1-positive tumor cells are widely validated and used as predictive biomarkers to select the patients for immune checkpoint blockade therapy [38]. However, different diagnostic anti-PD-L1 mAb clones were approved for specific therapeutic ones by FDA. For instance, clone 22C3 has been utilized as a predictive biomarker for pembrolizumab in several cancers. A clone 28-8 has been approved as a complementary assay for nivolumab. Each clone has a different cut-off point and cancer-specific scoring algorithm [2]. Both 22C3 and 28-8 recognize the extracellular domain of PD-L1, and exhibit similar subcellular patterns of PD-L1 expression in tumor and immune cells [2]. However, different staining patterns by 22C3 and 28-8 are also reported [39].

In this study, we developed novel dPD-L1 mAbs (L1Mab-352 and L1Mab-354) using peptide immunization of the intracellular domain, and showed the usefulness for immunohistochemical analysis in paraffin-embedded dPD-L1-positive cells (Figures 3 and 4). Further studies are essential to show whether L1Mab-352 and L1Mab-354 apply to formalin-fixed paraffin-embedded canine tumors. An anti-dPD-L1 mAb (6C11-3A11) which recognizes the extracellular domain of dPD-L1 was reported to apply to immunohistochemistry [17]. The comparison of the staining pattern of mAbs targeting dPD-L1 extracellular and intracellular domains could provide supportive information in human cancer diagnosis.

Currently, several anti-dPD-L1 mAbs have been developed for canine tumor therapy [16,17,40]. Like human tumors, standardization of PD-L1 immunohistochemistry will be required in the future.

Author Contributions: T.O. and T.T. performed the experiments. M.K.K. and Y.K. designed the experiments. T.O., H.S., and Y.K. analyzed the data. T.O. and H.S. wrote the manuscript. All authors read and approved the final manuscript and agreed to be accountable for all aspects of the research in ensuring that the accuracy or integrity of any part of the work is appropriately investigated and resolved. All authors have read and agreed to the published version of the manuscript.

Funding: This research was supported in part by the Japan Agency for Medical Research and Development (AMED) under grant nos. JP22ama121008 (to Y.K.), JP22am0401013 (to Y.K.), 23bm1123027h0001 (to Y.K.), JP22ck0106730 (to Y.K.), and JP21am0101078 (to Y.K.), and by the Japan Society for the Promotion of Science (JSPS) Grants-in-Aid for Scientific Research (KAKENHI), grant nos. 21K20789 (to T.T.), 22K06995 (to H.S.), 21K07168 (to M.K.K.), and 22K07224 (to Y.K.).

Institutional Review Board Statement: The animal study protocol was approved by the Animal Care and Use Committee of Tohoku University (Permit number: 2022MdA-001) for studies involving animals.

Informed Consent Statement: Not applicable.

Data Availability Statement: All related data and methods are presented in this paper. Additional inquiries should be addressed to the corresponding authors.

Conflicts of Interest: The authors declare no conflict of interest involving this article.

References

1. Alturki, N.A. Review of the Immune Checkpoint Inhibitors in the Context of Cancer Treatment. J Clin Med 2023, 12, doi:10.3390/jcm12134301.
2. Vranic, S.; Gatalica, Z. PD-L1 testing by immunohistochemistry in immuno-oncology. Biomol Biomed 2023, 23, 15-25, doi:10.17305/bjbms.2022.7953.
3. Paz-Ares, L.; Ciuleanu, T.E.; Cobo, M.; Schenker, M.; Zurawski, B.; Menezes, J.; Richardet, E.; Bennouna, J.; Felip, E.; Juan-Vidal, O.; et al. First-line nivolumab plus ipilimumab combined with two cycles of chemotherapy in patients with non-small-cell lung cancer (CheckMate 9LA): an international, randomised, open-label, phase 3 trial. Lancet Oncol 2021, 22, 198-211, doi:10.1016/S1470-2045(20)30641-0.
4. Baas, P.; Scherpereel, A.; Nowak, A.K.; Fujimoto, N.; Peters, S.; Tsao, A.S.; Mansfield, A.S.; Popat, S.; Jahan, T.; Antonia, S.; et al. First-line nivolumab plus ipilimumab in unresectable malignant pleural mesothelioma (CheckMate 743): a multicentre, randomised, open-label, phase 3 trial. Lancet 2021, 397, 375-386, doi:10.1016/S0140-6736(20)32714-8.
5. Diaz, L.A., Jr.; Shiu, K.K.; Kim, T.W.; Jensen, B.V.; Jensen, L.H.; Punt, C.; Smith, D.; Garcia-Carbonero, R.; Benavides, M.; Gibbs, P.; et al. Pembrolizumab versus chemotherapy for microsatellite instability-high or mismatch repair-deficient metastatic colorectal cancer (KEYNOTE-177): final analysis of a randomised, open-label, phase 3 study. Lancet Oncol 2022, 23, 659-670, doi:10.1016/S1470-2045(22)00197-8.
6. Freeman, G.J.; Long, A.J.; Iwai, Y.; Bourque, K.; Chernova, T.; Nishimura, H.; Fitz, L.J.; Malenkovich, N.; Okazaki, T.; Byrne, M.C.; et al. Engagement of the PD-1 immunoinhibitory receptor by a novel B7 family member leads to negative regulation of lymphocyte activation. J Exp Med 2000, 192, 1027-1034, doi:10.1084/jem.192.7.1027.
7. Collins, M.; Ling, V.; Carreno, B.M. The B7 family of immune-regulatory ligands. Genome Biol 2005, 6, 223, doi:10.1186/gb-2005-6-6-223.
8. Kreileder, M.; Barrett, I.; Bendtsen, C.; Brennan, D.; Kolch, W. Signaling Dynamics Regulating Crosstalks between T-Cell Activation and Immune Checkpoints. Trends Cell Biol 2021, 31, 224-235, doi:10.1016/j.tcb.2020.12.001.
9. Chan, A.C.; Irving, B.A.; Fraser, J.D.; Weiss, A. The zeta chain is associated with a tyrosine kinase and upon T-cell antigen receptor stimulation associates with ZAP-70, a 70-kDa tyrosine phosphoprotein. Proc Natl Acad Sci U S A 1991, 88, 9166-9170, doi:10.1073/pnas.88.20.9166.
10. Weiss, A. T cell antigen receptor signal transduction: a tale of tails and cytoplasmic protein-tyrosine kinases. Cell 1993, 73, 209-212, doi:10.1016/0092-8674(93)90221-b.
11. Sheppard, K.A.; Fitz, L.J.; Lee, J.M.; Benander, C.; George, J.A.; Wooters, J.; Qiu, Y.; Jussif, J.M.; Carter, L.L.; Wood, C.R.; et al. PD-1 inhibits T-cell receptor induced phosphorylation of the ZAP70/CD3zeta signalosome and downstream signaling to PKCtheta. FEBS Lett 2004, 574, 37-41, doi:10.1016/j.febslet.2004.07.083.

12. Baioni, E.; Scanziani, E.; Vincenti, M.C.; Leschiera, M.; Bozzetta, E.; Pezzolato, M.; Desiato, R.; Bertolini, S.; Maurella, C.; Ru, G. Estimating canine cancer incidence: findings from a population-based tumour registry in northwestern Italy. BMC Vet Res 2017, 13, 203, doi:10.1186/s12917-017-1126-0.
13. Maekawa, N.; Konnai, S.; Okagawa, T.; Nishimori, A.; Ikebuchi, R.; Izumi, Y.; Takagi, S.; Kagawa, Y.; Nakajima, C.; Suzuki, Y.; et al. Immunohistochemical Analysis of PD-L1 Expression in Canine Malignant Cancers and PD-1 Expression on Lymphocytes in Canine Oral Melanoma. PLoS One 2016, 11, e0157176, doi:10.1371/journal.pone.0157176.
14. Maekawa, N.; Konnai, S.; Takagi, S.; Kagawa, Y.; Okagawa, T.; Nishimori, A.; Ikebuchi, R.; Izumi, Y.; Deguchi, T.; Nakajima, C.; et al. A canine chimeric monoclonal antibody targeting PD-L1 and its clinical efficacy in canine oral malignant melanoma or undifferentiated sarcoma. Sci Rep 2017, 7, 8951, doi:10.1038/s41598-017-09444-2.
15. Choi, J.W.; Withers, S.S.; Chang, H.; Spanier, J.A.; De La Trinidad, V.L.; Panesar, H.; Fife, B.T.; Sciammas, R.; Sparger, E.E.; Moore, P.F.; et al. Development of canine PD-1/PD-L1 specific monoclonal antibodies and amplification of canine T cell function. PLoS One 2020, 15, e0235518, doi:10.1371/journal.pone.0235518.
16. Igase, M.; Nemoto, Y.; Itamoto, K.; Tani, K.; Nakaichi, M.; Sakurai, M.; Sakai, Y.; Noguchi, S.; Kato, M.; Tsukui, T.; et al. A pilot clinical study of the therapeutic antibody against canine PD-1 for advanced spontaneous cancers in dogs. Sci Rep 2020, 10, 18311, doi:10.1038/s41598-020-75533-4.
17. Maekawa, N.; Konnai, S.; Nishimura, M.; Kagawa, Y.; Takagi, S.; Hosoya, K.; Ohta, H.; Kim, S.; Okagawa, T.; Izumi, Y.; et al. PD-L1 immunohistochemistry for canine cancers and clinical benefit of anti-PD-L1 antibody in dogs with pulmonary metastatic oral malignant melanoma. NPJ Precis Oncol 2021, 5, 10, doi:10.1038/s41698-021-00147-6.
18. Deguchi, T.; Maekawa, N.; Konnai, S.; Owaki, R.; Hosoya, K.; Morishita, K.; Nakamura, M.; Okagawa, T.; Takeuchi, H.; Kim, S.; et al. Enhanced Systemic Antitumour Immunity by Hypofractionated Radiotherapy and Anti-PD-L1 Therapy in Dogs with Pulmonary Metastatic Oral Malignant Melanoma. Cancers (Basel) 2023, 15, doi:10.3390/cancers15113013.
19. Yamada, S.; Itai, S.; Nakamura, T.; Yanaka, M.; Kaneko, M.K.; Kato, Y. Detection of high CD44 expression in oral cancers using the novel monoclonal antibody, C(44)Mab-5. Biochem Biophys Rep 2018, 14, 64-68, doi:10.1016/j.bbrep.2018.03.007.
20. Tamura, R.; Oi, R.; Akashi, S.; Kaneko, M.K.; Kato, Y.; Nogi, T. Application of the NZ-1 Fab as a crystallization chaperone for PA tag-inserted target proteins. Protein Sci 2019, 28, 823-836, doi:10.1002/pro.3580.
21. Fujii, Y.; Matsunaga, Y.; Arimori, T.; Kitago, Y.; Ogasawara, S.; Kaneko, M.K.; Kato, Y.; Takagi, J. Tailored placement of a turn-forming PA tag into the structured domain of a protein to probe its conformational state. J Cell Sci 2016, 129, 1512-1522, doi:10.1242/jcs.176685.
22. Fujii, Y.; Kaneko, M.; Neyazaki, M.; Nogi, T.; Kato, Y.; Takagi, J. PA tag: a versatile protein tagging system using a super high affinity antibody against a dodecapeptide derived from human podoplanin. Protein Expr Purif 2014, 95, 240-247, doi:10.1016/j.pep.2014.01.009.
23. Kato, Y.; Kaneko, M.K.; Kuno, A.; Uchiyama, N.; Amano, K.; Chiba, Y.; Hasegawa, Y.; Hirabayashi, J.; Narimatsu, H.; Mishima, K.; et al. Inhibition of tumor cell-induced platelet aggregation using a novel anti-podoplanin antibody reacting with its platelet-aggregation-stimulating domain. Biochem Biophys Res Commun 2006, 349, 1301-1307, doi:10.1016/j.bbrc.2006.08.171.
24. Chalise, L.; Kato, A.; Ohno, M.; Maeda, S.; Yamamichi, A.; Kuramitsu, S.; Shiina, S.; Takahashi, H.; Ozone, S.; Yamaguchi, J.; et al. Efficacy of cancer-specific anti-podoplanin CAR-T cells and oncolytic herpes virus G47Delta combination therapy against glioblastoma. Mol Ther Oncolytics 2022, 26, 265-274, doi:10.1016/j.omto.2022.07.006.
25. Ishikawa, A.; Waseda, M.; Ishii, T.; Kaneko, M.K.; Kato, Y.; Kaneko, S. Improved anti-solid tumor response by humanized anti-podoplanin chimeric antigen receptor transduced human cytotoxic T cells in an animal model. Genes Cells 2022, 27, 549-558, doi:10.1111/gtc.12972.
26. Tamura-Sakaguchi, R.; Aruga, R.; Hirose, M.; Ekimoto, T.; Miyake, T.; Hizukuri, Y.; Oi, R.; Kaneko, M.K.; Kato, Y.; Akiyama, Y.; et al. Moving toward generalizable NZ-1 labeling for 3D structure determination with optimized epitope-tag insertion. Acta Crystallogr D Struct Biol 2021, 77, 645-662, doi:10.1107/S2059798321002527.
27. Kaneko, M.K.; Ohishi, T.; Nakamura, T.; Inoue, H.; Takei, J.; Sano, M.; Asano, T.; Sayama, Y.; Hosono, H.; Suzuki, H.; et al. Development of Core-Fucose-Deficient Humanized and Chimeric Anti-Human

Podoplanin Antibodies. Monoclon Antib Immunodiagn Immunother 2020, 39, 167-174, doi:10.1089/mab.2020.0019.

28. Abe, S.; Kaneko, M.K.; Tsuchihashi, Y.; Izumi, T.; Ogasawara, S.; Okada, N.; Sato, C.; Tobiume, M.; Otsuka, K.; Miyamoto, L.; et al. Antitumor effect of novel anti-podoplanin antibody NZ-12 against malignant pleural mesothelioma in an orthotopic xenograft model. Cancer Sci 2016, 107, 1198-1205, doi:10.1111/cas.12985.
29. Kaneko, M.K.; Abe, S.; Ogasawara, S.; Fujii, Y.; Yamada, S.; Murata, T.; Uchida, H.; Tahara, H.; Nishioka, Y.; Kato, Y. Chimeric Anti-Human Podoplanin Antibody NZ-12 of Lambda Light Chain Exerts Higher Antibody-Dependent Cellular Cytotoxicity and Complement-Dependent Cytotoxicity Compared with NZ-8 of Kappa Light Chain. Monoclon Antib Immunodiagn Immunother 2017, 36, 25-29, doi:10.1089/mab.2016.0047.
30. Ito, A.; Ohta, M.; Kato, Y.; Inada, S.; Kato, T.; Nakata, S.; Yatabe, Y.; Goto, M.; Kaneda, N.; Kurita, K.; et al. A Real-Time Near-Infrared Fluorescence Imaging Method for the Detection of Oral Cancers in Mice Using an Indocyanine Green-Labeled Podoplanin Antibody. Technol Cancer Res Treat 2018, 17, 1533033818767936, doi:10.1177/1533033818767936.
31. Shiina, S.; Ohno, M.; Ohka, F.; Kuramitsu, S.; Yamamichi, A.; Kato, A.; Motomura, K.; Tanahashi, K.; Yamamoto, T.; Watanabe, R.; et al. CAR T Cells Targeting Podoplanin Reduce Orthotopic Glioblastomas in Mouse Brains. Cancer Immunol Res 2016, 4, 259-268, doi:10.1158/2326-6066.CIR-15-0060.
32. Kuwata, T.; Yoneda, K.; Mori, M.; Kanayama, M.; Kuroda, K.; Kaneko, M.K.; Kato, Y.; Tanaka, F. Detection of Circulating Tumor Cells (CTCs) in Malignant Pleural Mesothelioma (MPM) with the "Universal" CTC-Chip and An Anti-Podoplanin Antibody NZ-1.2. Cells 2020, 9, doi:10.3390/cells9040888.
33. Nishinaga, Y.; Sato, K.; Yasui, H.; Taki, S.; Takahashi, K.; Shimizu, M.; Endo, R.; Koike, C.; Kuramoto, N.; Nakamura, S.; et al. Targeted Phototherapy for Malignant Pleural Mesothelioma: Near-Infrared Photoimmunotherapy Targeting Podoplanin. Cells 2020, 9, doi:10.3390/cells9041019.
34. Kato, Y.; Kaneko, M.K.; Kunita, A.; Ito, H.; Kameyama, A.; Ogasawara, S.; Matsuura, N.; Hasegawa, Y.; Suzuki-Inoue, K.; Inoue, O.; et al. Molecular analysis of the pathophysiological binding of the platelet aggregation-inducing factor podoplanin to the C-type lectin-like receptor CLEC-2. Cancer Sci 2008, 99, 54-61, doi:10.1111/j.1349-7006.2007.00634.x.
35. Kato, Y.; Vaidyanathan, G.; Kaneko, M.K.; Mishima, K.; Srivastava, N.; Chandramohan, V.; Pegram, C.; Keir, S.T.; Kuan, C.T.; Bigner, D.D.; et al. Evaluation of anti-podoplanin rat monoclonal antibody NZ-1 for targeting malignant gliomas. Nucl Med Biol 2010, 37, 785-794, doi:10.1016/j.nucmedbio.2010.03.010.
36. Kubli, S.P.; Berger, T.; Araujo, D.V.; Siu, L.L.; Mak, T.W. Beyond immune checkpoint blockade: emerging immunological strategies. Nat Rev Drug Discov 2021, 20, 899-919, doi:10.1038/s41573-021-00155-y.
37. Das, S.; Johnson, D.B. Immune-related adverse events and anti-tumor efficacy of immune checkpoint inhibitors. J Immunother Cancer 2019, 7, 306, doi:10.1186/s40425-019-0805-8.
38. Akhtar, M.; Rashid, S.; Al-Bozom, I.A. PD-L1 immunostaining: what pathologists need to know. Diagn Pathol 2021, 16, 94, doi:10.1186/s13000-021-01151-x.
39. Rimm, D.L.; Han, G.; Taube, J.M.; Yi, E.S.; Bridge, J.A.; Flieder, D.B.; Homer, R.; West, W.W.; Wu, H.; Roden, A.C.; et al. A Prospective, Multi-institutional, Pathologist-Based Assessment of 4 Immunohistochemistry Assays for PD-L1 Expression in Non-Small Cell Lung Cancer. JAMA Oncol 2017, 3, 1051-1058, doi:10.1001/jamaoncol.2017.0013.
40. Oh, W.; Kim, A.M.J.; Dhawan, D.; Kirkham, P.M.; Ostafe, R.; Franco, J.; Aryal, U.K.; Carnahan, R.H.; Patsekin, V.; Robinson, J.P.; et al. Development of an Anti-canine PD-L1 Antibody and Caninized PD-L1 Mouse Model as Translational Research Tools for the Study of Immunotherapy in Humans. Cancer Res Commun 2023, 3, 860-873, doi:10.1158/2767-9764.CRC-22-0468.